European Radiology (2019) 29:6982–6990
https://doi.org/10.1007/s00330-019-06321-6

UROGENITAL

Dynamic contrast-enhanced MR imaging of the prostate: intraindividual comparison of gadoterate meglumine and gadobutrol

Chau Hung Lee[1,2] · Balamurugan Vellayappan[3] · Matthias Taupitz[1] · Bernd Hamm[1] · Patrick Asbach[1]

Received: 6 December 2018 / Revised: 27 May 2019 / Accepted: 11 June 2019 / Published online: 1 July 2019

Abstract

Objectives To intraindividually compare the signal-enhancing effect of 0.5 M gadoterate meglumine and 1.0 M gadobutrol in dynamic contrast-enhanced magnetic resonance (DCE-MR) imaging of the prostate.

Methods Fifty patients who underwent two 3-T MR examinations of the prostate were included in this IRB-approved retrospective uncontrolled, unrandomized study. All received two scans (mean time interval, 20.5 months) including T1-weighted DCE-MR imaging, one with 0.5 M gadoterate meglumine and one with 1.0 M gadobutrol. Equimolar doses of gadolinium (0.1 mmol/kg body weight) were administered with identical injection speed (2 mL/s), resulting in differing gadolinium delivery rate. An identical region of interest (ROI_{tz}) within a BPH-node was identified on both scans. The area under the time-enhancement curve of each ROI_{tz} from 0 to 180 s post contrast arrival and pharmacokinetic parameters were calculated. Relative enhancement and signal-to-noise (SNR) and contrast-to-noise (CNR) ratios in the delayed phase at about 180 s were compared between both agents.

Results There was a significantly larger area under the time-enhancement curve (5.53 vs 4.97 $p = 0.0007$) and higher relative enhancement of BPH nodules (2.23 vs 1.96 $p < 0.0001$) with gadobutrol compared with gadoterate meglumine. There were no significant differences in SNR (44.55 vs 37.63 $p = 0.12$), CNR (31.22 vs 26.39 $p = 0.18$), and pharmacokinetic parameters Ktrans (0.31 vs 0.32 $p = 0.86$), Ve (1.36 vs 0.98 $p = 0.13$), and Kep (0.34 vs 0.36 $p = 0.12$).

Conclusions At equimolar doses, increased gadolinium delivery over time using gadobutrol provides higher relative enhancement parameters in BPH nodules compared with gadoterate meglumine, but does not translate into improved SNR or CNR.

Key Points

- *At equal injection rate and equimolar total dose, gadobutrol compared with gadoterate meglumine provides a significantly greater relative enhancement in DCE-MR imaging of BPH over the first 180 s.*
- *There are no significant differences in SNRs, CNRs, and pharmacokinetic parameters between the two GBCAs.*

Keywords Prostate · Magnetic resonance imaging · Contrast media · Gadobutrol · Gadoterate meglumine

✉ Chau Hung Lee
chau_hung_lee@ttsh.com.sg

[1] Department of Radiology, Charité– Universitätsmedizin Berlin, corporate member of Freie Universität Berlin, Humboldt-Universität zu Berlin, and Berlin Institute of Health, Campus Benjamin Franklin, Berlin, Germany

[2] Department of Radiology, Tan Tock Seng Hospital, 11 Jalan Tan Tock Seng, Singapore 308433, Singapore

[3] Department of Radiation Oncology, National University Cancer Institute, National University Health System, Singapore, Singapore

Abbreviations

AUC_{enh}	Area under the RE-t curve from contrast agent arrival time to 180 s after arrival
BPH	Benign prostatic hyperplasia
CNR	Contrast-to-noise ratio
DCE-MR	Dynamic contrast-enhanced magnetic resonance
GBCA	Gadolinium-based contrast agent
GRAPPA	GeneRalized Autocalibrating Partial Parallel Acquisition
IRB	Institutional Review Board
Kep	Flux rate constant

Ktrans	Volume transfer constant reflecting the efflux rate of gadolinium contrast from blood plasma into the interstitial space
MR	Magnetic resonance
RE	Relative enhancement
RE-t	Relative enhancement over time
ROI_{tz}	Region of interest corresponding to a BPH nodule in the transition zone
SNR	Signal-to-noise ratio
t_{180}	Time point closest to 180 s after first DCE-MR acquisition
TE	Echo time
TR	Repetition time
Ve	Extravascular extracellular space corresponding to the interstitial space

Introduction

Gadolinium-based contrast agents (GBCA) containing macrocyclic gadolinium complexes such as gadoterate meglumine or gadobutrol are commonly used in magnetic resonance (MR) imaging. Due to higher kinetic stability of macrocyclic agents and improved clearance, linear compounds have been phased out in many countries [1].

Gadobutrol is manufactured at double the gadolinium concentration of gadoterate meglumine (1 M vs 0.5 M). T1 molar relaxivity of gadobutrol (5 L/mmol s), although showing slight inter-study variability, is generally higher compared with gadoterate meglumine (3.5 L/mmol s) at 3 T in bovine plasma [2]. Given these differences in physiochemical properties, there has been an interest in comparing the two GBCAs in multiphasic and dynamic contrast-enhanced MR (DCE-MR) imaging. This involves repeated acquisition of the target anatomy before, during, and after intravenous administration of a GBCA. In addition, for DCE-MR imaging, pharmacokinetic parameters such as tissue capillary permeability (Ktrans), extracellular volume ratio (Ve), and flux rate constant (Kep) can then be extracted using pharmacokinetic models, such as the Tofts model [3, 4].

In previous interindividual comparative studies, gadobutrol has been shown to provide greater enhancement compared with gadoterate meglumine and gadopentetate dimeglumine in MR imaging of brain, breast, and prostate malignancies [5–7]. An intraindividual comparison would reduce interindividual variability and increase statistical power. At our institution, both gadobutrol and gadoterate meglumine are routinely used in DCE-MR imaging of the prostate with no preference or specific selection criteria for either GBCA. We therefore performed a retrospective intraindividual head-to-head comparison of gadobutrol and gadoterate meglumine in DCE-MR imaging of the prostate.

Materials and methods

Study design and patient cohort

Approval was obtained from our institution's ethical review board, for access to patient's existing imaging studies and electronic medical records. Informed consent was waived as there was no direct patient contact, no impact on patient care, and imaging and medical records were de-identified for analysis. A search of our institution's Picture Archiving and Communication System (PACS) database was performed for the period of August 2011 to September 2017. Patient demographics, MR imaging protocol, dose of administered GBCA, time interval between scans, diagnosis of prostate cancer, and treatment related to prostate cancer or benign prostatic hyperplasia (BPH) were noted. Patients were included if (a) they had two MR scans of the prostate performed with both GBCAs, gadoterate meglumine and gadobutrol, at equimolar dose adjusted to body weight (0.1 mmol/kg body weight) and (b) both scans showed BPH with similar morphology, allowing exact spatial matching. If a patient had more than two scans, the scans performed within the closest time interval from one another were analysed. Patients were excluded if (a) there was biopsy-proven prostatic malignancy, (b) prior prostate-related treatment (radiotherapy, immunotherapy, hormonal therapy, BPH treatment) or extensive post-biopsy changes involving transition zone (arbitrarily defined as haemorrhage involving more than half of the transitional zone rendering assessment of BPH nodules difficult), (c) scanning parameters differed between the two DCE-MR imaging scans (excluding differences in temporal resolution and number of time points), (d) doses of the two GBCAs were not equimolar, or (e) if no BPH nodule could be identified on both scans. From a patient list generated from the PACS database, all potential scans were reviewed in consensus, consecutively, for suitability by two radiologists (with 4 and 10 years of experience in urogenital imaging, respectively). If there was a discrepancy between the two radiologists, with regard to the inclusion and exclusion criteria for a patient, that patient was excluded. In this fashion, suitable patients who met the inclusion criteria were selected consecutively, by "going down the list" (convenience sampling), until the desired cohort size was achieved.

A minimum cohort size of 19 patients (38 paired scans) was determined by power calculation, further described in the "Statistical analysis" subsection. A final cohort of 50 patients (100 paired scans) was selected (Fig. 1). All 50 patients underwent the first MR scans for raised serum prostate-specific antigen (PSA) defined as > 4 ng/mL by our institution's laboratory reference values. Twenty-one patients had a negative transrectal ultrasound-guided systematic prostate biopsy prior to the first scan, while the other 29 patients were biopsy-naive at the time of the first MR scan. Clinical

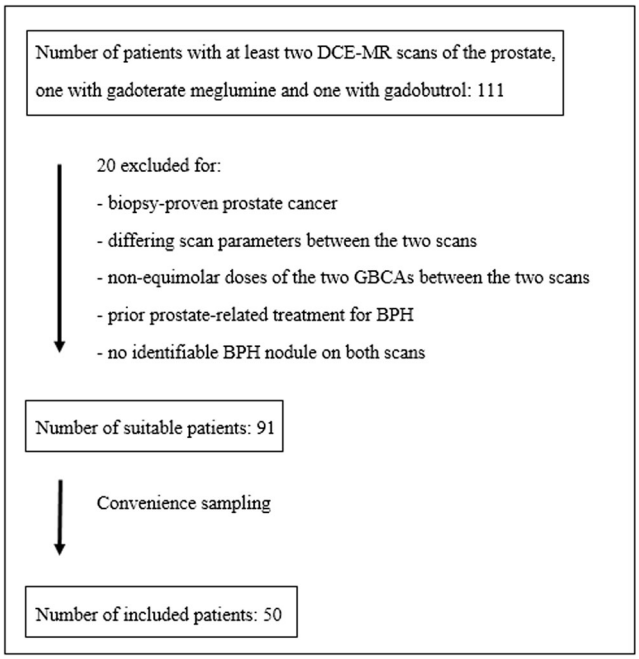

Fig. 1 Patient selection process. Retrospective non-randomised intraindividual study of men undergoing at least two DCE-MR scans of the prostate, one performed with gadoterate meglumine and one performed with gadobutrol

indications for the second scans were persistently rising serum PSA (48 patients), new palpable prostatic nodule on digital rectal examination (1 patient), and follow-up of subcentimetre PI-RADS 4 peripheral zone lesion with a negative targeted biopsy after the first scan (1 patient). In 47 patients, the scans with gadoterate meglumine were performed before the scans with gadobutrol. The mean volume of gadoterate meglumine administered was 16.8 mL (13 to 30 mL) and the mean volume of gadobutrol administered was 8.4 mL (6.3 to 13 mL), maintaining equimolar gadolinium dose of 0.1 mmol/kg body weight for all scans. The mean patient age at the time of the scans performed with gadoterate meglumine was 62.8 years (43 to 82 years) and the mean patient age at the time of the scans performed with gadobutrol was 64.4 years (45 to 83 years). The mean interval between the two scans was 20.5 months (1 to 50 months).

DCE-MR imaging technique

All scans included in the analysis were performed at 3 T (Magnetom Skyra, Siemens Healthineers). A combination of a 6-element phased-array body matrix surface coil (Siemens Healthineers) placed ventrally over the pelvic region and a 24-element spine matrix coil (Siemens Healthineers) integrated into the scan table was used. All scans were performed on one MR scanner using identical coils. No major software upgrades or hardware upgrades were identified from February 2013 (earliest included scan) until September 2017 (latest included scan), ensuring identical MR imaging conditions as best as possible of all evaluated scans.

DCE-MR imaging of the whole prostate was performed with the following scan parameters: T1-weighted 3-dimensional time-resolved angiography (3D-TWIST) sequence in the axial oblique plane, slice thickness 3 mm, field of view 260 mm with spatial coverage from prostatic apex to seminal vesicles, flip angle 12°, repetition time (TR) 4.83 ms, echo time (TE) 1.87 ms, matrix size 192 × 133, parallel imaging factor (GRAPPA) of 2 in the phase-encoding direction, receiver bandwidth 260 Hz/pixel, temporal resolution of 3.9 s to 6 s (depending on the number of slices acquired per volume), and 50 to 70 time points. The view-sharing technique was set to acquire 51% of the central k-space (acquired at every time point) and a 20% sampling density of the peripheral k-space. After 5 pre-contrast acquisitions, 0.1 mmol/kg body weight of GBCA, either gadoterate meglumine (Dotarem, Guerbet) or gadobutrol (Gadovist, Bayer Schering) was administered intravenously via a 22-G cannula in an antecubital vein at a rate of 2 mL/s, followed by a normal saline bolus chaser of 20 mL at 2 mL/s, both using an automated power injector (Medrad Spectris Solaris, Bayer). In addition, the pre-contrast dataset was subtracted section by section from all datasets at each subsequent time point after contrast administration using evaluation software (Syngo, Siemens), to obtain a set of subtracted images.

The remaining MR sequences not subject to investigation in this analysis included small field-of-view axial and coronal oblique T2-weighted fast spin-echo sequences, axial oblique diffusion-weighted imaging (acquired *b*-values 0, 50, 500, 1000 s/mm^2; calculated *b*-value 1400 s/mm^2) as well as large field-of-view true axial T1-weighted spin-echo sequence of the whole pelvis.

Image analysis and quantitative assessment

Lesion identification

For both MR examinations of each patient, an arbitrary time point in the delayed phase that corresponds closest to 180 s after the first time point acquisition was selected (t_{180}). In our study, we define the delayed phase as that part of the time-enhancement curve after the initial rapid rise in relative enhancement. In conjunction with the T2-weighted sequences, a BPH nodule was identified in the transition zone on the DCE-MR images at t_{180} on both scans of each patient. A circular region of interest (ROI_{tz}) marker was positioned manually at the largest diameter of the BPH nodule on one image slice on the DCE-MR imaging sequence. The ROI_{tz} from one scan was copied onto the second scan of the same patient, ensuring identical size. Small adjustments were made for minor differences in angulation and positions between the two scans to ensure that the morphologically identical BPH nodules on

both scans were encompassed by the ROI_{tz}. Care was taken not to include areas of susceptibility or T1-hyperintensity within the ROI_{tz}. The same 2 radiologists who identified the patient cohort retrospectively read the scans and identified the ROI_{tz} in consensus.

Parameters recorded

The following parameters were subsequently recorded for each ROI_{tz}:

1. Enhancement curve type. Relative enhancement-time (RE-t) curves were generated based on the 3D-TWIST sequence using evaluation software (Tissue 4-D software analysis, Syngo, Siemens). The curves were classified into type I (progressive increase in enhancement), type II (plateau), and type III (wash-out with a gradual decrease in enhancement after a peak) [8]. The curve type was identified visually.
2. Area under the RE-t curve from the time of GBCA arrival to 180 s after arrival (AUC_{enh}). This predetermined time interval accommodated differences in temporal resolution, GBCA arrival time, and acquisition time between DCE-MR imaging scans. AUC_{enh} was used as a measure of total relative enhancement across all included time points.
3. Pharmacokinetic parameters (Ktrans, Ve, Kep). Evaluation software (Tissue 4-D software analysis, Syngo, Siemens) was used to derive Ktrans and Ve. This was based on the simplified one-compartment Toft's model from which Kep was then calculated using the formula Kep = Ktrans/Ve [9].
4. Relative enhancement (RE) of the ROI_{tz} at t_{180}. $RE = (S_c - S_{nc})/S_{nc}$ (S_c, average signal intensity of the ROI_{tz} at t_{180}; SI_{nc}, average signal intensity of the ROI_{tz} in the 2nd pre-contrast acquisition).
5. Signal-to-noise ratio (SNR) and contrast-to-noise ratio (CNR). Image noise was assessed using the difference method, given the application of parallel imaging and use of multi-array surface coils [10]. Applying this method (where image noise N = standard deviation across baseline image frames), the image slices containing the same ROI_{tz} at the 2nd and 3rd pre-contrast acquisitions were identified. The subtracted image, reflecting the signal difference in the ROI_{tz} between these two time points, was obtained using subtraction software (Syngo, Siemens). The same circular ROI_{tz} was then copied onto this subtracted image for each scan. The same circular marker was also copied onto one of the obturator internus muscles of the same image slice containing the ROI_{tz} at t_{180}. Image noise was defined as the standard deviation of the signal in the ROI_{tz} on the subtracted image (SD_{noise}). $SNR = (S_c - S_{nc})/SD_{noise}$ and $CNR = (S_c - S_m)/SD_{noise}$ (S_m, average signal intensity of the obturator internus muscle at t_{180}).

Statistical analysis

The sample size was estimated using a 2-sample, 2-sided equality test ($\alpha = 0.05$, $\beta = 0.8$) and assuming a 12% increase in average peak relative enhancement produced by gadobutrol in normal peripheral zone based on the interindividual prospective study of Durmus et al [7]. Therefore, at least 19 subjects (38 paired scans) were needed. The RE-t curves were fitted using nonlinear, nonparametric models [11]. AUC_{enh} for each ROI_{tz} was derived from the fitted curves. Curve fitting and derivation of AUC_{enh} were performed using MATLAB version R2013a (Mathworks). Curve types identified for the two GBCAs (parameter 1) were presented as frequency and compared using the chi-squared test. To compare the two GBCAs for parameters 2 to 5, a two-sided Wilcoxon signed-rank test was performed.

Findings were presented as means with 95% confidence intervals. The significance level for all comparisons was set at 5%. Statistical analysis was performed using SPSS Statistics for Windows, version 21.0 (IBM Corp.).

Results

There was no significant difference in enhancement curve types between the two GBCAs ($p = 0.19$) (Table 1).

As specifically assessed in BPH nodules in our study, gadobutrol produced higher total relative enhancement compared with gadoterate meglumine with a significantly larger mean AUC_{enh} (5.53 vs 4.97, $p = 0.0007$) (Fig. 2). In the delayed phase (at a selected time point closest to 180 s after the first acquisition of DCE-MR imaging), there was significantly higher RE with gadobutrol compared with gadoterate meglumine (2.23 vs 1.96, $p < 0.05$) (Table 2).

There were no significant differences between the two GBCAs in terms of SNR and CNR ($p = 0.12$ and $p = 0.18$, respectively) as well as the pharmacokinetic parameters Ktrans ($p = 0.86$), Ve ($p = 0.13$), and Kep ($p = 0.12$) (Table 2).

Table 1 Distribution of curve types between gadoterate meglumine and gadobutrol, assessed visually in consensus by two radiologists. The curves were classified into type I (progressive increase in enhancement), type II (plateau), and type III (gradual decrease in enhancement after a peak). There was no significant difference in curve types between the two GBCAs

Curve type	Gadobutrol	Gadoterate meglumine	*p* value
I	6 (12%)	2 (4%)	0.19
II	37 (74%)	36 (72%)	
III	7 (14%)	12 (24%)	

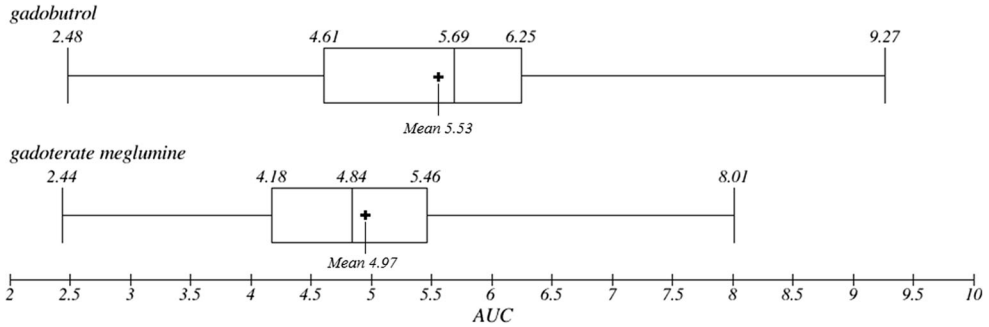

Fig. 2 Comparison of the area under the RE-t curve from 0 to 180 s post contrast arrival (AUC_{enh}) between all scans performed with gadoterate meglumine and with gadobutrol. The box plot indicates higher total relative enhancement with gadobutrol compared with gadoterate meglumine. Minimum and maximum AUC_{enh} are shown. The middle 50% is indicated as median with mean indicated as "+". The whiskers extending to 25th and 75th percentiles

Figures 3 and 4 show the marking of the ROI_{tz}, the RE-t curves, and calculation of AUC_{enh} for the MR examinations performed with gadoterate meglumine (Fig. 3) and gadobutrol (Fig. 4) in the same patient. The scans were performed 14 months apart, and the first scan was performed with gadoterate meglumine.

Discussion

T1 molar relaxivity of GBCAs is an important factor in contrast-enhanced MR imaging, which is commonly T1-weighted. Our study showed that gadobutrol produces greater overall enhancement compared with gadoterate meglumine in DCE-MR imaging of the prostate, as evaluated in benign BPH tissue. This could be due to a higher T1 molar relaxivity or higher gadolinium delivery rate (given the same contrast injection rate for all scans in our study), or a combination of both. Compared with other GBCAs approved for clinical use, gadobutrol has higher T1 molar relaxivity and is manufactured at twice molar concentration (1 M vs 0.5 M) [12]. This would theoretically generate a higher signal in tissues at the same gadolinium dose. The higher T2 molar relaxivity of gadobutrol at 3 T could also influence the overall enhancement on DCE-MR imaging particularly in the first pass through the vascular system, although this is rarely observed at doses utilised in routine clinical practice [13].

Studies of conventional contrast-enhanced MR imaging of the brain, heart, and liver generally found gadobutrol to provide superior enhancement and signal compared with GBCAs with lower T1 molar relaxivities [14–17]. Studies of MR angiography have shown that, although gadobutrol may provide better signal-/contrast-to-noise ratio compared with gadoterate meglumine, reader rating of image quality, vessel visualisation, and preference were often variable [18–22]. In multiphasic MR mammography, gadobutrol has been shown to provide better enhancement or improved lesion delineation compared with gadoterate meglumine [6, 23, 24]. In the DETECT trial comparing two linear GBCAs gadobenate dimeglumine and gadopentetate dimeglumine for the detection of breast malignancy, gadobenate showed better diagnostic performance which investigators attributed to higher T1 molar relaxivity [25]. There is little published data comparing gadoterate meglumine and gadobutrol in DCE-MR imaging of the prostate. Durmus et al compared gadobutrol and gadopentetate dimeglumine (a GBCA with almost the same

Table 2 Mean values and 95% CI of parameters assessed to compare the two GBCAs. AUC_{enh} and relative enhancement at t_{180} in the ROI_{tz} were significantly higher for scans performed with gadobutrol compared with gadoterate meglumine, when administered at the same injection rate of 2 mL/s. There were no significant differences in the SNR and CNR as well as the pharmacokinetic parameters, between the two GBCAs when administered at the same injection rate

	Gadobutrol	Gadoterate meglumine	*p* value
AUC_{enh}	5.53 (95% CI 5.15, 5.91)	4.97 (95% CI 4.67, 5.27)	0.0007*
RE	2.23 (95% CI 2.09, 2.37)	1.96 (95% CI 1.84, 2.08)	< 0.0001*
SNR	44.55 (95% CI 38.38, 50.72)	37.63 (95% CI 33.61, 41.65)	0.12
CNR	31.22 (95% CI 26.54, 35.90)	26.39 (95% CI 23.04, 29.74)	0.18
Ktrans (min^{-1})	0.31 (95% CI 0.27, 0.35)	0.32 (95% CI 0.28, 0.36)	0.86
Ve	1.36 (95% CI 1.27, 1.45)	0.98 (95% CI 0.88, 1.08)	0.13
Kep (min^{-1})	0.34 (95% CI 0.27, 0.41)	0.36 (95% CI 0.32, 0.40)	0.12

*Significantly different parameters between gadoterate meglumine and gadobutrol

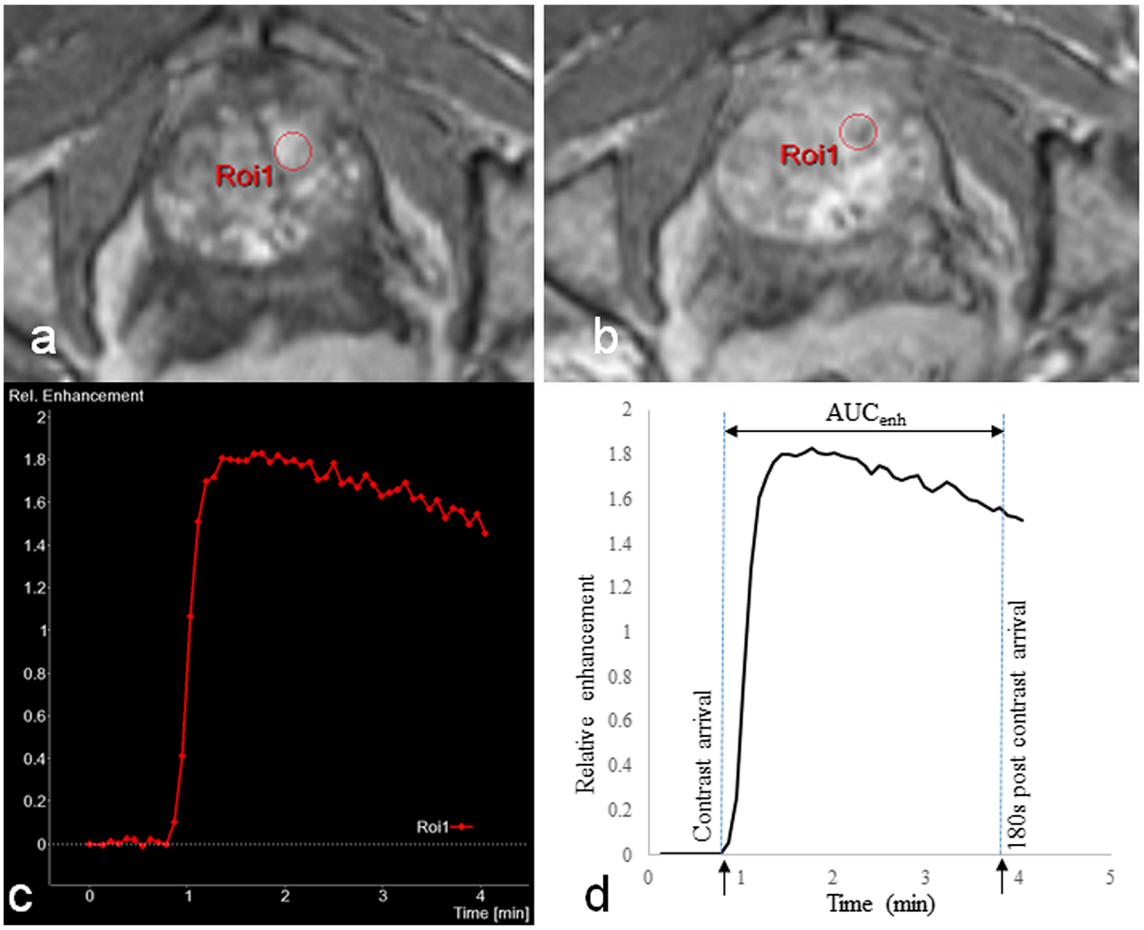

Fig. 3 Example in a selected patient illustrating marking of the ROI_{tz} in a DCE-MR imaging scan obtained with 16-mL gadoterate meglumine. This was a 73-year-old gentleman who presented with a raised serum PSA of 5.1 ng/mL. Systematic transrectal ultrasound biopsy was negative for malignancy. DCE-MR imaging was performed with a T1-weighted 3D-TWIST sequence. Fifty time points were acquired with a temporal resolution of 4.9 s and total acquisition time of 4 min and 2 s. A BPH nodule was identified in the transitional zone in the anterior part of the left midgland. **a** In the arterial phase, the BPH nodule showed early enhancement. **b** At t_{180}, the ROI_{tz} was marked for analysis. **c** The RE-t curve was generated. **d** Curve fitting was performed and AUC_{enh} was derived

T1 molar relaxivity as gadoterate meglumine) in DCE-MR imaging for the detection of prostate cancer and demonstrated significantly higher peak relative enhancement of prostate cancer using gadobutrol [7]. In that study, the comparison was interindividual. Our study, designed for intraindividual comparison, could complement findings from that study.

While it would have been optimal to analyse peak enhancement for our study, we were unable to determine a peak enhancement for most lesions, which showed type I or II enhancement curves, not unexpected in BPH [26, 27]. Instead, we analysed the area under the RE-t curves, a method extrapolated from drug concentration-time curve analysis in pharmacological drug studies [28]. Our results show that gadobutrol produces a significantly higher total relative enhancement compared with gadoterate meglumine as evidenced by a significantly larger area under the RE-t curve over 180 s post contrast arrival. Furthermore, we analysed the relative enhancement in the delayed phase beyond the initial wash-in slope of the RE-t curve, which also showed higher relative enhancement with gadobutrol compared with gadoterate meglumine. In our study, both gadoterate meglumine and gadobutrol were administered at the same rate of 2 mL/s, resulting in a higher rate of gadolinium delivery with gadobutrol (given its higher concentration). This has been shown to affect the first pass gadolinium concentration and bolus peak, influencing the initial "wash-in" slope of the time-enhancement curve and peak enhancement [29]. This could potentially confound our results. However, we attempted to mitigate this limitation at least partially, by assessing the RE-t curve over 180 s post contrast arrival and relative enhancement at a later time point in the delayed phase beyond the initial "wash-in" slope of the time-enhancement curve.

We did not demonstrate significant differences in SNR and CNR between the two GBCAs. This might be attributed to variations in SD_{noise} between the two examinations due to external factors such as magnetic field inhomogeneity, image processing, and patient motion while scan parameters were almost identical for the two examinations [30]. Studies

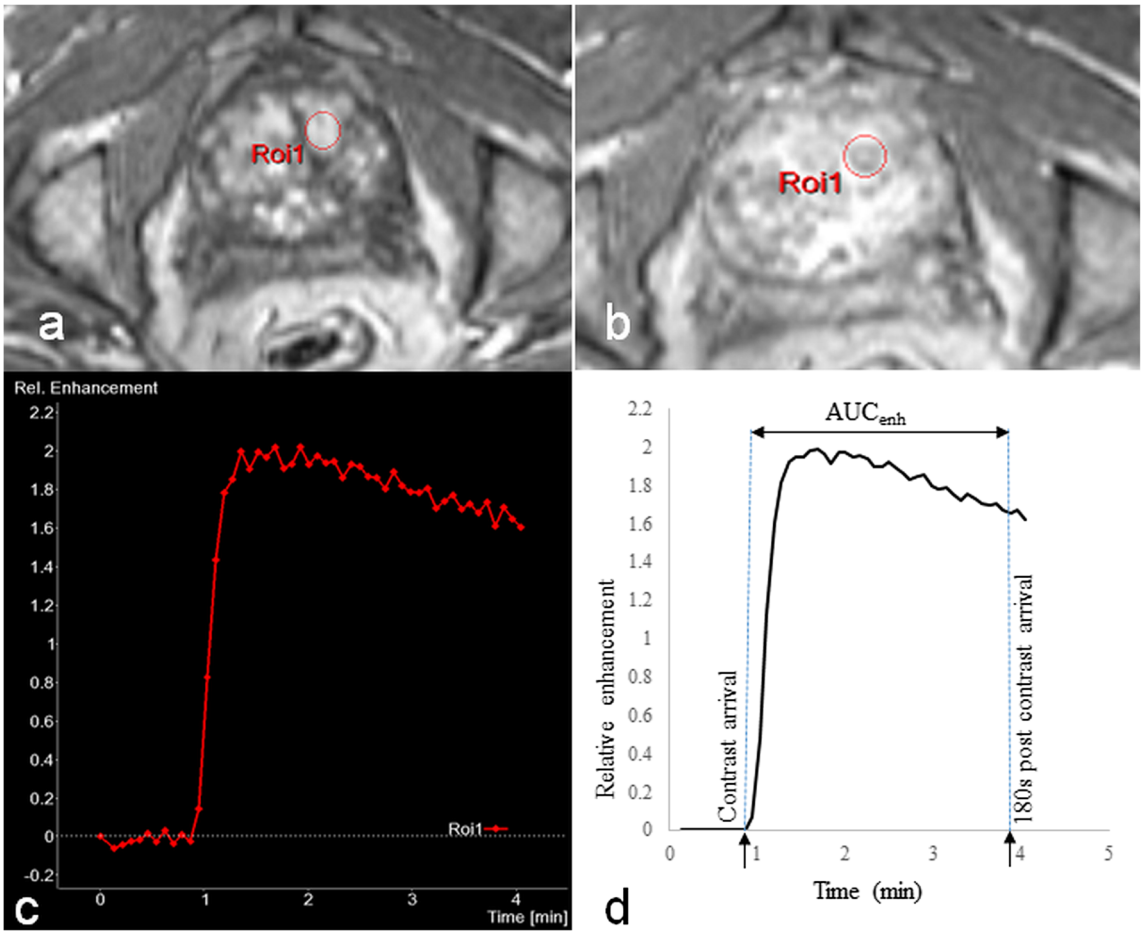

Fig. 4 Marking of the ROI_{tz} in a DCE-MR imaging scan obtained with 7.2-mL gadobutrol for the same patient as in Fig. 3, performed 14 months later. This was a 73-year-old gentleman who presented with a raised serum PSA of 5.1 ng/mL. Systematic transrectal ultrasound biopsy was negative for malignancy. This second scan was performed due to rising serum PSA. DCE-MR imaging was performed with a T1-weighted 3D-TWIST sequence. DCE-MR imaging was performed with the same number of time points (50), temporal resolution (4.9 s), and total acquisition time (4 min and 2 s). **a** In the arterial phase, the same BPH nodule as seen on the scan performed with gadoterate meglumine in Fig. 3, again showing early enhancement. **b** At t_{180}, the ROI_{tz} was marked for analysis. This was copied from the scan performed with gadoterate meglumine ensuring identical size. **c** Evaluation software was used to generate the RE-t curve. **d** Curve fitting was performed, and AUC_{enh} was derived as shown

comparing gadoterate meglumine and gadobutrol in terms of SNR and CNR yield variable results. Kim et al found a significantly higher SNR and CNR in small hepatomas with gadobutrol [31]. In lower limb MR angiography studies, Haneder et al [18] demonstrated a higher SNR and CNR with gadobutrol compared with gadoterate meglumine whereas Szucs-Farkas et al [19] did not find significant differences in SNR or CNR between the two GBCAs. There were no significant differences in SNR or CNR between the two GBCAs in the evaluation of brain tumours or osteomyelitis [5, 15, 32]. Thus, it can be concluded that the higher relative enhancement produced by gadobutrol does not necessarily translate into a higher SNR or CNR, and indirectly, overall better image quality. This might have implications for lesion detection in clinical practice. For example, one study comparing gadobutrol and gadopentetate dimeglumine in MR mammography for the detection of breast cancer in 400 women showed that, while there was significantly higher relative enhancement with gadobutrol, there was no significant difference in the number of malignant lesions detected [33]. It could also be possible that better delineation of lesion morphology in breast lesions, rather than increased enhancement, contributed to improved detection of malignant breast lesions [25].

Pharmacokinetic parameters (Ktrans, Ve, Kep) did not differ significantly between the two GBCAs. Therefore, the choice of either GBCA should not affect the pharmacokinetic maps generated by commercially available software.

This study has some limitations. With the significant time interval between the two MR examinations in each patient and the fact that most examinations with gadobutrol were performed after the examinations with gadoterate meglumine, the increased enhancement with gadobutrol might be influenced by other factors such as progression of BPH or changes in patient weight over time. The addition of a control region of

interest could reduce these confounding factors; however, identifying a completely normal prostate tissue on MR is challenging in the presence of BPH. Therefore, no control tissue was investigated. Also, given the same injection rate of both GBCAs, the increased enhancement with gadobutrol could be influenced by higher gadolinium delivery rate (given its higher concentration) rather than its higher T1 molar relaxivity, a factor we could not eliminate completely in our study.

We compared the enhancement of BPH nodules, which is arguably of little clinical relevance. Moreover, the distribution of negatively charged gadoterate meglumine and electrically neutral gadobutrol could be affected by negatively charged mucopolysaccharides in BPH tissue [34, 35]. However, it has been shown histologically that BPH tissue and prostate malignancy both contain mucins of similar negative charges [36–38], which would influence the distribution of the two GBCAs in a similar fashion. Furthermore, the overlap in enhancement patterns of BPH and prostate cancer is well established [39–41]. Therefore, our results might be applicable to prostate cancer.

Further, based on the Prostate Imaging Reporting and Data System (PI-RADS) version 2, there is less emphasis on the time-enhancement curve in DCE-MR imaging for detection of prostate cancer [42]. Superior enhancement of gadobutrol demonstrated in BPH might not translate into increased sensitivity for the detection of prostate malignancy, without taking into account corresponding T2-weighted and diffusion-weighted imaging. This is different from MR mammography, where enhancement plays a central role in breast cancer detection [43, 44].

Further studies prospectively comparing the two GBCAs to determine if the increased enhancement with gadobutrol improves detection of prostate cancer in clinical practice may be considered.

Conclusion

In this retrospective, non-randomised intraindividual study comparing gadoterate meglumine and gadobutrol with respect to their signal-enhancing properties in DCE-MR imaging of the prostate when administered at equimolar doses at the same injection rate, the higher gadolinium delivery of gadobutrol produces higher relative enhancement in DCE-MR imaging of the prostate compared with that of gadoterate meglumine, as assessed in BPH nodules. However, this advantage did not translate into better SNR or CNR.

Acknowledgements The authors would like to thank Ms. Bettina Herwig for language editing of the manuscript.

Funding The authors state that this work was partially-funded by the Deutsche Forschungsgemeinschaft (DFG, German Research Foundation) – SFB 1340/1 2018.

Compliance with ethical standards

Guarantor The scientific guarantor of this publication is Dr. Patrick Asbach.

Conflict of interest The authors of this manuscript declare no relationships with any companies, whose products or services may be related to the subject matter of the article.

Statistics and biometry One of the authors has significant statistical expertise.

Informed consent Written informed consent was waived by the Institutional Review Board.

Ethical approval Institutional Review Board approval was obtained.

Methodology
- retrospective
- observational
- performed at one institution

References

1. Bellin MF, Van Der Molen AJ (2008) Extracellular gadolinium-based contrast media: an overview. Eur J Radiol 66:160–167
2. Rohrer M, Bauer H, Mintorovitch J, Reguardt M, Weinmann HJ (2005) Comparison of magnetic properties of MRI contrast media solutions at different magnetic field strengths. Invest Radiol 40: 715–724
3. Cuenod CA, Balvay D (2013) Perfusion and vascular permeability: basic concepts and measurement in DCE-CT and DCE-MRI. Diagn Interv Imaging 94:1187–1204
4. Tofts PS (1997) Modeling tracer kinetics in dynamic Gd-DTPA MR imaging. J Magn Reson Imaging 7:91–101
5. Attenberger UI, Runge VM, Morelli JN, Williams J, Jackson CB, Michaely HJ (2010) Evaluation of gadobutrol, a macrocyclic, non-ionic gadolinium chelate in a brain glioma model: comparison with gadoterate meglumine and gadopentetate dimeglumine at 1.5 T, combined with an assessment of field strength dependence, specifically 1.5 versus 3 T. J Magn Reson Imaging 31:549–555
6. Fallenberg EM, Renz DM, Karle B et al (2015) Intraindividual, randomized comparison of the macrocyclic contrast agents gadobutrol and gadoterate meglumine in breast magnetic resonance imaging. Eur Radiol 25:837–849
7. Durmus T, Vollnberg B, Schwenke C et al (2013) Dynamic contrast enhanced MRI of the prostate: comparison of gadobutrol and Gd-DTPA. Rofo 85:862–868
8. Kulh CK, Mielcarek P, Klaschik S et al (1999) Dynamic breast MR imaging: are signal intensity time course data useful for differential diagnosis of enhancing lesions? Radiology 211:101–110
9. Tofts PS, Kermode AG (1991) Measurement of the blood-brain barrier permeability and leakage space using dynamic MR imaging. 1. Fundamental concepts. Magn Reson Med 17:357–367
10. Dietrich O, Raya JG, Reeder SB, Reiser MF, Schoenberg SO (2007) Measurement of signal-to-noise ratios in MR images: influence of multichannel coils, parallel imaging, and reconstruction filters. J Magn Reson Imaging 26:375–385
11. Motulsky HJ, Ransnas LA (1987) Fitting curves to data using nonlinear regression: a practical and nonmathematical review. FASEB J 1:365–374

12. Prince MR, Lee HG, Lee CH et al (2017) Safety of gadobutrol in over 23,000 patients: the GARDIAN study, a global multicentre, prospective, non-interventional study. Eur Radiol 27:286–295
13. Elster AD (1997) How much contrast is enough? Dependence of enhancement on field strength and MR pulse sequence. Eur Radiol 7:S276–S280
14. Anzalone N, Scarabino T, Venturi C et al (2013) Cerebral neoplastic enhancing lesions: multicenter, randomized, crossover intraindividual comparison between gadobutrol (1.0M) and gadoterate meglumine (0.5M) at 0.1 mmol Gd/kg body weight in a clinical setting. Eur J Radiol 82:139–145
15. Maravilla KR, San-Juan D, Kim SJ et al (2017) Comparison of gadoterate meglumine and gadobutrol in the MRI diagnosis of primary brain tumors: a double-blind randomized controlled intraindividual crossover study (the REMIND study). AJNR Am J Neuroradiol 38:1681–1688
16. Saake M, Langner S, Schwenke C et al (2016) MRI in multiple sclerosis: an intra-individual, randomized and multicentric comparison of gadobutrol with gadoterate meglumine at 3 T. Eur Radiol 26:820–828
17. Lancelot E, Froehlich J, Heine O, Desché P (2016) Effects of gadolinium-based contrast agent concentrations (0.5 M or 1.0 M) on the diagnostic performance of magnetic resonance imaging examinations: systematic review of the literature. Acta Radiol 57: 1334–1343
18. Haneder S, Attenberger UI, Schoenberg SO, Loewe C, Arnaiz J, Michaely HJ (2012) Comparison of 0.5 M gadoterate and 1.0 M gadobutrol in peripheral MRA: a prospective, single-center, randomized, crossover, double-blind study. J Magn Reson Imaging 36:1213–1221
19. Szucs-Farkas Z, Froehlich JM, Ulrich M et al (2008) 1.0-M gadobutrol versus 0.5-M gadoterate for peripheral magnetic resonance angiography: a prospective randomized controlled clinical trial. J Magn Reson Imaging 27:1399–1405
20. Kramer JH, Arnoldi E, François CJ et al (2013) Dynamic and static magnetic resonance angiography of the supra-aortic vessels at 3.0 T: intraindividual comparison of gadobutrol, gadobenate dimeglumine, and gadoterate meglumine at equimolar dose. Invest Radiol 48:121–128
21. Hoelter P, Lang S, Weibart M et al (2017) Prospective intraindividual comparison of gadoterate and gadobutrol for cervical and intracranial contrast-enhanced magnetic resonance angiography. Neuroradiology 59:1233–1239
22. Loewe C, Arnaiz J, Krause D, Marti-Bonmati L, Haneder S, Kramer U (2015) MR angiography at 3 T of peripheral arterial disease: a randomized prospective comparison of gadoterate meglumine and gadobutrol. AJR Am J Roentgenol 204:1311–1321
23. Renz DM, Durmus T, Böttcher J et al (2014) Comparison of gadoteric acid and gadobutrol for detection as well as morphologic and dynamic characterization of lesions on breast dynamic contrast-enhanced magnetic resonance imaging. Invest Radiol 49:474–484
24. Pediconi F, Catalano C, Padula S et al (2008) Contrast-enhanced MR mammography: improved lesion detection and differentiation with gadobenate dimeglumine. AJR Am J Roentgenol 191:1339–1346
25. Martincich L, Faivre-Pierret M, Zechmann CM et al (2011) Multicenter, double-blind, randomized, intraindividual crossover comparison of gadobenate dimeglumine and gadopentetate dimeglumine for breast MR imaging (DETECT trial). Radiology 258:396–408
26. Franiel T, Hamm B, Hricak H (2011) Dynamic contrast-enhanced magnetic resonance imaging and pharmacokinetic models in prostate cancer. Eur Radiol 21:616–626
27. De Visschere PJL, Vral A, Perletti G et al (2017) Multiparametric magnetic resonance imaging characteristics of normal, benign and malignant conditions in the prostate. Eur Radiol 27:2095–2109
28. Brown DL, Lalla CD, Masselink AJ (2013) AUC versus peak-trough dosing of vancomycin: applying new pharmacokinetic paradigms to an old drug. Ther Drug Monit 35:443–449
29. Tombach B, Benner T, Reimer P et al (2003) Do highly concentrated gadolinium chelates improve MR brain perfusion imaging? Intraindividually controlled randomized crossover concentration comparison study of 0.5 versus 1.0 mol/L gadobutrol. Radiology 226:880–888
30. Weishaupt D, Köchli VD, Marincek B (2003) Factors affecting the signal-to-noise ratio. In: How does MRI work? Springer, Berlin, pp 31–42
31. Kim YK, Lee YH, Kim CS, Han YM, Hwang SB (2008) Double-dose 1.0-M gadobutrol versus standard-dose 0.5-M gadopentetate dimeglumine in revealing small hypervascular hepatocellular carcinomas. Eur Radiol 18:70–77
32. Pennekamp W, Roggenland D, Hering S et al (2011) Intraindividual, randomised comparison of the MRI contrast agents gadobutrol and gadoterate in imaging the distal lower limb of patients with known or suspected osteomyelitis, evaluated in an off-site blinded read. Eur Radiol 21:1058–1067
33. Escribano F, Sentís M, Oliva JC et al (2018) Dynamic magnetic resonance imaging of the breast: comparison of gadobutrol vs. Gd-DTPA. Radiologia 60:49–56
34. Frenzel T, Lengsfeld P, Schirmer H, Hütter J, Weinmann HJ (2008) Stability of gadolinium-based magnetic resonance imaging contrast agents in human serum at 37 degrees C. Invest Radiol 43:817–828
35. Gillis A, Gray M, Burstein D (2002) Relaxivity and diffusion of gadolinium agents in cartilage. Magn Reson Med 48:1068–1071
36. Wiener E, Woertler K, Weirich G, Rummeny EJ, Settles M (2007) Contrast enhanced cartilage imaging: comparison of ionic and non-ionic contrast agents. Eur J Radiol 63:110–119
37. Mathur SK, Gupta S, Marwah N, Narula A, Singh S, Arora B (2003) Significance of mucin stain in differentiating benign and malignant lesions of prostate. Indian J Pathol Microbiol 46:593–595
38. Khanna A, Patil R, Deshmukh A (2014) Assessment of the potential of pathological stains in human prostate cancer. J Clin Diagn Res 8:124–128
39. Chesnais AL, Niaf E, Bratan F et al (2013) Differentiation of transitional zone prostate cancer from benign hyperplasia nodules: evaluation of discriminant criteria at multiparametric MRI. Clin Radiol 68:e323–e330
40. van Niekerk CG, Witjes JA, Barentsz JO, van der Laak JA, Hulsbergen-van de Kaa CA (2013) Microvascularity in transition zone prostate tumors resembles normal prostatic tissue. Prostate 73: 467–475
41. Lemaitre L, Puech P, Poncelet E et al (2009) Dynamic contrast-enhanced MRI of anterior prostate cancer: morphometric assessment and correlation with radical prostatectomy findings. Eur Radiol 19:470–480
42. Purysko AS, Rosenkrantz AB, Barentsz JO, Weinreb JC, Macura KJ (2016) PI-RADS version 2: a pictorial update. Radiographics 36:1354–1372
43. Drew PJ, Chatterjee S, Turnbull LW et al (1999) Dynamic contrast enhanced magnetic resonance imaging of the breast is superior to triple assessment for the pre-operative detection of multifocal breast cancer. Ann Surg Oncol 6:599–603
44. Pickles MD, Lowry M, Manton DJ, Turnbull LW (2015) Prognostic value of DCE-MRI in breast cancer patients undergoing neoadjuvant chemotherapy: a comparison with traditional survival indicators. Eur Radiol 25:1097–1106